# MAGIC POLYMER GEL DOSIMETRY USING X-RAY COMPUTED TOMOGRAPHY: A FEASIBILITY STUDY

by

MOHAMMAD ABDALLA MOHAMMAD ALJAMAL

**Thesis submitted in fulfilment of the requirements for the degree of Master of science (Medical Radiation)**

**June 2008**

## DEDICATION

I would like to dedicate my thesis to my parents, whose confidence in me has been unwavering, and to my beloved brother and sisters. Thank you for the moral and financial support that kept me afloat.

## ACKNOWLEDGEMENTS

First of all, I would like to thank Allah for giving me the strength and courage to persevere throughout the duration of this research project.

I wish to acknowledge with greatest thanks to my father Mr. Abdalla Mohammad Aljamal whom has been my source of inspiration because of his continuous support and encouragement. My lovely mother who has dedicated all her life with sweat and blood to her sons. My brother, Ahmad and my sisters whom has showed me their determination in which gave me confidence to pursue my work and research.

I would like to express my utmost gratitude to my main supervisor, Associate Professor Dr. Ahmad Zakria and to my co-supervisor, Dr. Shaharum Shamsuddin for their untiring dedication, brilliant knowledge of research, exceptional advice, leadership, ideas, support ,encouragement and constructive comments throughout writing which without them none of this research could have take place.

My deepest thanks go to Mr. Nik Ruzman for his advice and support during irradiation process and special thanks to Mr. Zaky bin Harun for his support during my scanning process.

I would like to extend my grateful appreciation and thanks to all my friends, for their friendship, unlimited help and support especially, Dr. Najeeb Abu Alroub, Dr. Kareem, Dr. Naeem, , Dr. Zyiad kammal, Dr. Muath, Aidin Molouki , Suliman Tayseer, Venue ,Khairul Azan, Amir, Khari,.

Lastly, but not the least, I would like to thank all my fellow colleagues and friends who have directly or indirectly participated in making this study possible. While it might be not possible to name them all here, their help is forever unforgettable.

# TABLE OF CONTENTS

**CHAPTER TWO: MATERIALS AND METHODS**

# LIST OF TABLES

# LIST OF FIGURES

## LIST OF ABBREVIATIONS

| | |
|---|---|
| Am-241 | Amersham 241 |
| BANG | BIS Acrylamide Nitrogen Gelatin |
| CT | Computed Tomography |
| HPLC | High Performance Liquid Chromatography |
| HU | Hounsfield Unit |
| HUSM | Hospital University Sains Malaysia |
| IMRT | Intensity Modulated Radiotherapy |
| LAC | Linear Attenuation Coefficient |
| MAGAT | Methacrylic acid Gelatin and Tetrakis |
| MAGIC | Methacrylic and Ascorbic acids in Gelatin Initiated by Copper |
| MCA | Multi Channel Analyzer |
| MRI | Magnetic Resonance imaging |
| NIH | National Institutes of Health |
| OCT | Optical Computed Tomography |
| OD | Optical Density |
| PAG | Polyacrylamide Gelatin |
| PAGAT | Polyacrylamide Gelatin and Tetrakis |
| PDD | Percentage Depth Dose |
| ROI | Region of Interest |
| SD | Standard deviation |
| SNR | Signal to Noise Ratio |
| SRS | Stereotactic radiosurgery |

| | |
|---|---|
| SRT | Stereotactic radiotherapy |
| SSD | Source to Surface Distance |
| THP | Tetrakis phosphonium Chloride |
| TLD | Thermoluminescent Dosimeter |
| TPS | Treatment Planning System |
| US | Ultrasound |

# DOSIMETRI GEL POLIMER MAGIC MENGGUNAKAN TOMOGRAFI BERKOMPUTER SINAR-X : SATU KAJIAN KEBOLEHLAKSANAAN

## ABSTRAK

Projek ini bertujuan mengkaji kebolehlaksanaan pembangunan sistem dosimetri gel polimer MAGIC ("Methacrylic and Ascorbic acid in Gelatin Initiated by Copper") menggunakan "helical multislice" tomografi berkomputer sinar-X di HUSM untuk menentukan taburan dos. Gel MAGIC disediakan mengikut formula yang telah dicadangkan oleh Fong *et al.* (2001) dengan sedikit perubahan. Gel ini dikaji untuk melihat samada ia mempunyai ciri-ciri yang sama dengan air. Prinsip Archimedes digunakan untuk menentukan kepadatan jisim ($\rho$) dan sementara itu pengiraan pecahan berat kandungan elemen dan nombor atomik efektif ($Z_{eff}$) gel juga dilakukan. Kepadatan elektron juga diukur pada suhu bilik dengan sudut serakan 90°. Pemalar pengecilan linear ($\mu$) gel yang tidak disinari, gel disinari dan air ditentukan dengan menggunakan sumber Am-241 berdasarkan prinsip alur sempit. Ukuran pemalar pengecilan linear gel MAGIC yang tidak disinari dan air adalah $0.84 \pm 0.04$ cm $^{-1}$ dan $0.85 \pm 0.02$ $cm^{-1}$ masing-masing. Keputusan ini menunjukkan bahawa gel polimer MAGIC adalah setara dengan air. Data yang didapati dari gel yang disinari menunjukkan wujudnya hubungan linear antara koefisien pengecilan linear dan dos bagi julat 2 ke 40 Gy. Protokol pengimejan CT untuk menghasilkan imej gel disinari yang paling berkualiti telah ditentukan bagi mendapatkan nilai dos. Gel disinari yang diletakkan di dalam fantom silinder mengandungi air diimbas dengan menggunakan parameter imbasan yang sedia ada (kV, mA, dan 'reconstruction algorithm') dengan keluasan medan 25 x 25 $cm^2$ dan ketebalan hirisan 5mm.

Nisbah isyarat terhadap hingar (SNR) dan sisihan piawai (SD) adalah parameter yang dipilih untuk menentukan kualiti imej selepas proses pemurataan imej dilakukan. Imej yang paling berkualiti ialah imej yang mempunyai SNR tertinggi dan SD terendah dan parameter imbasan yang sejajar digunakan sebagai protokol untuk mengimbas gel dipersinarkan. Protokol imbasan dimana parameter imbasannya adalah 140 kV dan 400 mA dengan ketebalan hirisan 5 mm, masa dedahan 1000 ms, 'standard reconstruction algorithm' dan dengan keluasan medan 25 x 25 $cm^2$ menhasilkan imej yang paling berkualiti. Protokol imbasan ini digunakan untuk mengambil imej gel MAGIC disinari dengan pelbagai dos untuk menentukan hubungan antara purata nombor CT dan dos. Di dapati hubungan antara nombor purata CT dan dos adalah linear antara 2 – 40 Gy di mana nombor CT (HU) –dos sensitiviti adalah 0.30 ± 0.02 HU $Gy^{-1}$. Bagi mengesahkan kegunaan gel dosimetri berasaskan CT untuk mengukur dos, peratusan dos kedalaman (PDD) dan lengkung isodos (profil alur) bagi alur foton berukuran 8 x 8 $cm^2$ dari pemecut linear 6 MV diukur. Pebandingan dibuat antara PDD dan lengkung isodos yang telah diukur dengan apa yang telah dikira di dalam air menggunakan komputer perancangan rawatan radioterapi (TPS). Ketidakakuran PDD gel disinari berbanding TPS pada kedalaman 5 cm dan 10 cm adalah masing-masing ±1.8% dan ±2.1%. Maksimum ketidakakuran PDD gel disinari berbanding dengan kiraan TPS di dalam air adalah ±3%. Maksimum ketidakakuran lengkung isodos gel berbanding dengan kiraaan TPS di dalam air pada kedalaman 5 cm dan 10 cm adalah masing-masing ±10% dan 11.6%.

Kesimpulannya, keputusan menunjukkan bahawa sistem dosimetri gel MAGIC berasaskan CT menggunakan pengimbas CT di HUSM boleh menentukan dos foton bertenaga tinggi dalam julat 2-40 Gy.

# MAGIC POLYMER GEL DOSIMETRY USING X-RAY COMPUTED TOMOGRAPHY: A FEASIBILITY STUDY

## ABSTRACT

The aim of this project is to carry out the feasibility study of developing MAGIC (Methacrylic and Ascorbic acid in Gelatin Initiated by Copper) polymer gel dosimetry system by utilising helical multislice X-ray computed tomography (CT) available in HUSM to determine dose. The MAGIC gel was prepared based on the formulation proposed in the literature by Fong *et al.* (2001) with some modifications. The characteristics of the gel were studied for its water-equivalent properties. The mass density ($\rho$) was determined based on Archimedes' principle. The weight fraction of elemental composition and the effective atomic number ($Z_{eff}$) were calculated. The electron density was also measured with 90 degree scattering angle at room temperature. The linear attenuation coefficient ($\mu$) of unirradiated gel, irradiated gel, and water were determined using Am-241 based on narrow beam geometry. The measured linear attenuation coefficient of unirradiated MAGIC gel and water was found to be $0.84 \pm 0.04$ $cm^{-1}$ and $0.85 \pm 0.02$ $cm^{-1}$ respectively. The results showed that the MAGIC gel is water-equivalent. The data obtained using irradiated gel showed a linear relationship between linear attenuation coefficient and absorbed dose in the range 2 to 40 Gy. The protocol for CT imaging to obtain the best quality image of irradiated MAGIC gel was determined for evaluating dose information. The irradiated gel placed inside the cylindrical water phantom was scanned using various available scan parameters (kV, mA and reconstruction algorithm) with the field of view 25 x 25 $cm^2$ and 5 mm slice thickness.

The signal to noise ratio (SNR) and standard deviation (SD) were the parameters chosen to determine the image quality after image averaging process was carried out. The image which has the highest SNR and lowest SD was the best quality image and the corresponding scan parameters were used as our protocol for scanning the irradiated gel. The scan parameters of 140 kV and 400 mA with 5 mm slice thickness, 1000 ms exposure time, standard reconstruction algorithm and 25 x 25 $cm^2$ field of view were chosen as scanning protocol. Using this scanning protocol, the irradiated MAGIC gels of different doses were imaged to establish relation between average CT numbers and doses. A linear relation was found between average CT numbers and doses in the range of 2-40 Gy with CT number (HU)-dose sensitivity of 0.30 ± 0.02 HU $Gy^{-1}$. In order to verify the usefulness of the CT based gel dosimetry to measure dose, the percentage depth dose (PPD) and isodose curve (beam profile) of 8 x 8$cm^2$ field size photon beam from 6 MV linear accelerator were measured. The measured PDD and isodose curves were compared with that calculated in water using radiotherapy treatment planning computer system (TPS). The disagreement of irradiated gel PDD compare to TPS at 5 cm and 10 cm depth were found to be ±1.8%, ±2.1% respectively. The maximum disagreement of gel PDD compare to TPS calculation in the water was ±3%. The maximum disagreement of gel isodose curves compare to TPS calculation in the water at 5 cm and 10 cm measurements were ±10%, ±11.6% respectively. The results show that the CT based MAGIC gel dosimetry system using HUSM CT scanner could determine the dose of high energy photon in the range 2-40 Gy.

# CHAPTER ONE

# INTRODUCTION

## 1.1 Deposition and Measurement of Dose

In radiotherapy dose may be deposited by electrons, γ-rays, X-rays, protons, neutrons and a number of other heavy charged particles. These particles are classed as ionizing radiation, which is any radiation that has the ability to ionize atoms of the matter through which it passes. The minimum energy required to eject an electron from an atom is approximately 4 eV. Therefore, any particle that possesses kinetic energy greater than 4 eV is considered to be an "ionizing radiation". Similarly, photons whose energies are greater than 4 eV can be considered to be "ionizing radiation". Ionizing radiation can be further sub-divided into two groups: directly and indirectly ionizing radiation. Charged particles are considered to be directly ionizing radiation since they have the ability to disrupt the atomic structure through which they travel and produce chemical and biological changes. Conversely, X-rays and γ-rays are classified as indirectly ionizing radiation because they do not directly cause biological and chemical damage, but they can produce charged particles that will in turn produce damage.

### 1.1.1 Interaction of ionizing radiation with the matter

Dose is deposited through the interactions of ionizing radiation with matter. A brief discussion will be provided on the mechanisms of interaction for both indirectly and directly ionizing radiation with matter.

### 1.1.1.1 Interactions of Indirectly Ionizing Radiation with Matter

In radiological physics there are three main types of interactions of γ-ray and X-ray photons with matter that have to be considered. These are the Compton effect, the Photoelectric effect and pair production.

These three interactions result in the transfer and deposition of energy to the medium. The cross section of any interaction is a measure of the probability of that interaction occurring. Each of these interactions, by way of its cross section, contributes to the coefficients of mass attenuation ($\mu/\rho$), mass-energy transfer ($\mu_{tr}/\rho$), and mass-energy absorption ($\mu_{en}/\rho$) coefficients. These interactions will be discussed in more detail below.

The probability of each of these interactions occurring is dependent on the energy of the beam and $Z_{eff}$, the electron-fraction-weighted-average atomic number of the atoms in the absorbing material (Attix, 1986). The $Z_{eff}$ of water is 7.42 whereas the $Z_{eff}$ of the gel dosimeter is approximately 7.31 (De Deen *et al.,* 2006). For such Iow values of Z and for photons in the range 20 keV to 30 MeV, the Compton effect is dominant, as shown in Figure 1.1.

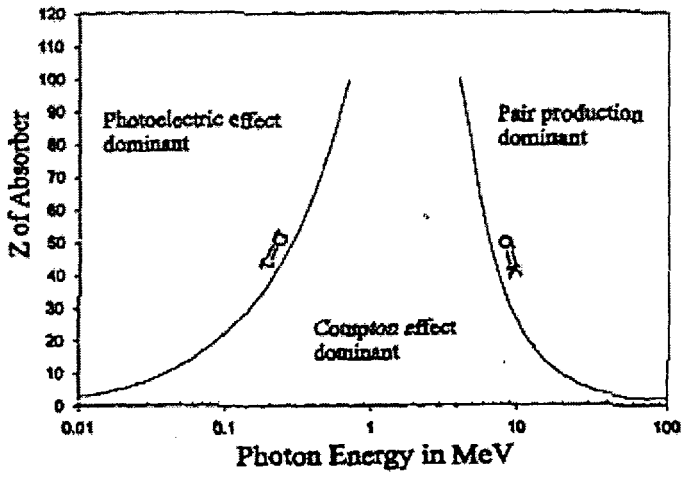


**Figure 1.1. A diagram representing the relative importance of the three main interactions in radiological physics, the Compton effect, photoelectric effect and pair production. The curve on the left hand-side indicates where the photoelectric mass attenuation coefficient, $\tau/p$, equals the Compton mass attenuation coefficient,$\sigma/p$ .Similarly, the right hand-side curve is where the Compton mass attenuation coefficient, $\sigma/p$, equals the pair production mass attenuation coefficient, $k/p$ (adapted from Attix, 1986)**

### 1.1.1.1(a) The Compton Effect

The Compton effect describes the interaction which an incident photon gives up part of its energy to a weakly bound electron, causing the electron to be ejected from the atom. The incident photon is then scattered, as shown in Figure 1.2, with energy that is equal to that of the original quantum less the recoil energy of the electron.

The Compton interaction probability is governed by the Klein-Nishina (K-N) cross section, which is heavily dependent on the energy of the incident photon beam ($h\nu$) and photon scattering angle $\theta$.

The Compton mass attenuation coefficient, $\sigma/\rho$, is given by:

$$\frac{\sigma}{\rho} = \frac{N_A Z}{A} {}_e\sigma \quad \ldots\ldots\ldots\ldots\ldots (1.1)$$

Where $N_A$ is Avogadro's number, A is the average mass number of the nuclei in the material, Z is the average atomic number, and ${}_e\sigma$ is the total K-N cross section per electron.

The energy transfer coefficient, $(\sigma_{tr}/\rho)$, describes the amount of energy that is transferred to the recoil electron. This term is determined from a modification of the differential K-N cross section and yields $({}_e\sigma_{tr}/\rho)$, the K-N energy-transfer coefficient. The Compton mass energy transfer coefficient can now be written as:

$$\frac{\sigma}{\rho} = \frac{N_A Z}{A} {}_e\sigma_{tr} \quad \ldots\ldots\ldots\ldots\ldots (1.2)$$

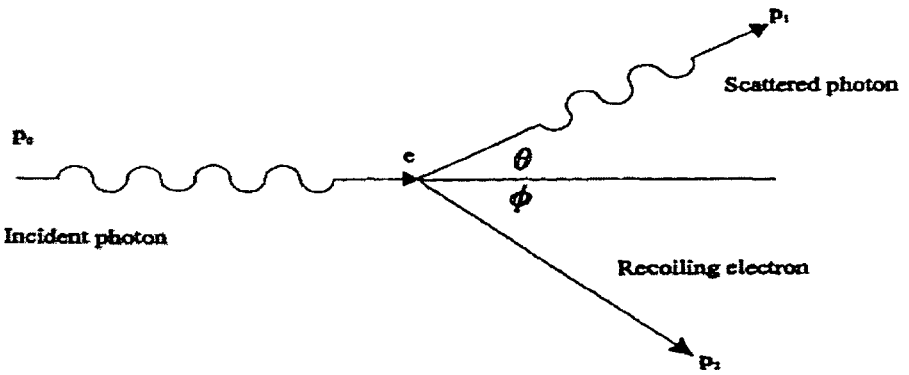


**Figure 1.2. A schematic diagram of the Compton effect. An incident with moment, $p_0$, strikes a stationary electron which then recoils with momentum $p_2$. The scattered photon departs with momentum $p_1$ (Attix, 1986)**

### 1.1.1.1(b) The Photoelectric Effect

The photoelectric effect describes the interaction that occurs when an incident photon relinquishes all of its energy to an atomic electron. The electron atomic subsequently ejected from the atom, as shown in Figure 1.3. The energy of the electron is that of the incident photon minus the binding energy of the electron.

The cross section for the photoelectric effect is not easily derived and most tables consist of values obtained from experimental data. In the energy region in which the photoelectric effect is dominant, that is for energies less than about 0.1 MeV.

The photoelectric mass attenuation coefficient, $\tau/\rho$, is found to be proportional to $(Z/h\nu)^3$, i.e.:

$$\tau/\rho \propto (Z/h\nu)^3 \quad \ldots\ldots\ldots\ldots\ldots\ldots (1.3)$$

where $h\nu$ is the energy of the incident photon.

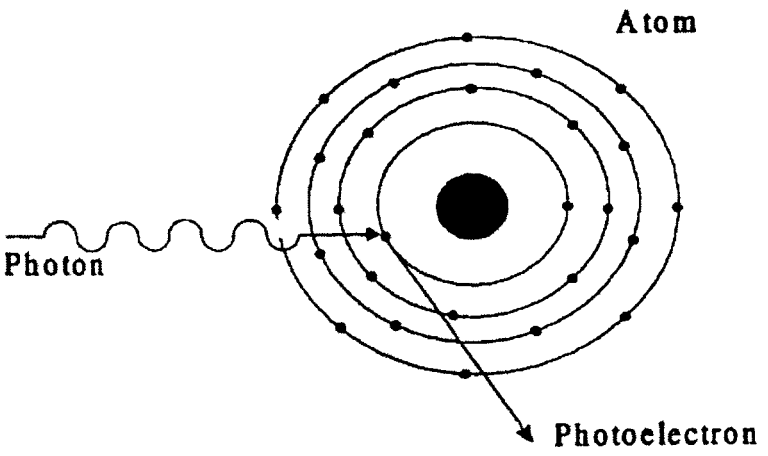


**Figure 1.3 The photoelectric effect (William, 2005)**

### 1.1.1.1(c) Pair Production

For water equivalent material and for photons whose energy is greater than 1.02 MeV, there is a probability that the photon will be completely absorbed through the mechanism of pair production. Pair production occurs when a photon passes near the nucleus of an atom and is subject to strong nuclear fields. The photon may suddenly disappear and emerge as a positron-electron pair, as shown in Figure 1.4. Charge is conserved because the lepton pair has opposite charges. Any energy in excess of 1.02 MeV is shared between the pair. Energy and momentum cannot be conserved simultaneously.

Therefore, when discussing the production of a positron-electron pair, only energy is conserved and when one includes the nucleus into the system, only momentum is conserved. The probability of pair production occurring, measured by the pair production coefficient, K, is proportional to $Z^2$ per atom or to Z per electron or per gram.

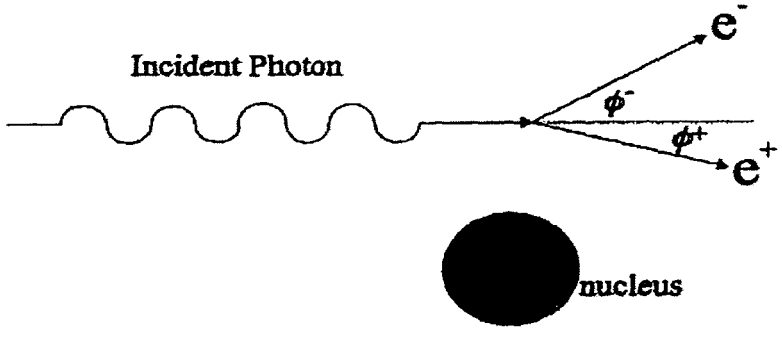


**Figure 1.4 Schematic of pair production. An incident photon, passing through the Coulomb force field of an atomic nucleus, vanishes giving rise to a positron-electron pair (Khan, 1994)**

### 1.1.1.2 Interactions of Directly Ionizing Radiation with Matter

Unlike indirectly ionizing radiation, the chance of interactions of charged particles occurring with matter is considerably greater due to the Coulomb-force field that surrounds the particles. A charged particle will interact with the electrons and nuclei of atom in the immediate in its path. With each of these interactions, only a fraction of the charged particle's initial kinetic energy is relinquished, and the particle therefore interacts with many atoms before coming to rest. The term path- length describes the length of the path that these particles take through matter. Another term, range, describes the expected distance that these particles will travel before eventually coming to rest. Because of the nature of these particles, their paths are not usually straight, and not even identical particles will follow the same path. For electrons, especially, since their mass is quite small, there is a considerable amount of scattering within the medium.

The interactions of charged particles with matter can be divided into three main categories: soft collisions, hard collisions, and coulomb-force interactions with the external nuclear field. These three interactions are incorporated into the expression for the mass stopping power, used to describe the rate at which energy is lost per unit length: (dT / pdx) Y, T, Z; Y, T, Z signifying that it is heavily dependent on the type of particle, Y, the particle's kinetic energy, T, and the Z of the material. The mass stopping power is usually measured in MeV $cm^2g^{-1}$.

The mass stopping power is usually further divided into the mass collision stopping power, subscript c, and the mass radiative stopping power, subscript r :

$$\left(\frac{dT}{\rho dx}\right)=\left(\frac{dT}{\rho dx}\right)_c+\left(\frac{dT}{\rho dx}\right)_r \quad \ldots\ldots\ldots\ldots\ldots (1.4)$$

The mass radiative stopping power describes the rate at which bremsstrahlung is produced by electrons and positrons. Bremsstrahlungs, also known as braking radiation, are X-rays produced as the electron or positron decelerates (Attix 1986). Only electrons and positrons produce bremsstrahlung due to their small mass. The mass radiative stopping power term is essentially zero for other charged particles. So-called soft collisions occur when the closest distance of approach, or the impact parameter, is several atomic radii or greater. In this interaction the Coulomb force field of the charged particle affects the atom as a whole. The consequence is that the atom is either excited to a higher energy level or becomes ionized through the ejection of a valence electron. Only a small fraction of the charged particle's energy is transferred to the absorbing matter in a single interaction. But because large numbers of such interactions occur, they account for more than half of the energy transferred to the absorbing matter.

Hard collisions, also known as "knock-on" collisions, occur with the electrons in an atom when the impact parameter of the particles is on the order of the atomic radius. These electrons are ejected from their orbits with a considerable amount of energy. These ejected electrons are called delta rays (δ-rays). Also, characteristic X-rays and/or Auger electrons can be produced if the ejected electron originates from an inner shell. The fraction of energy dissipated via this interaction is comparable to that of the soft collision interactions, even though its probability is much less than that of soft collisions.

When a charged particle approaches the nucleus of an atom, the particle is scattered either elastically, resulting in no energy loss, or inelastically, resulting in the ejection of an X-ray photon. This interaction occurs most frequently with electrons. Due to the high percentage of the interactions that result in elastic scattering, the electrons follow very tortuous paths. This tendency increases with large Z and causes substantial backscattering. When the interaction results in inelastic scattering, which occur a very small percentage of the time, a significant amount of energy is given up which results in the production of bremsstrahlung.

## 1.2 Measurement of Dose

The traditional dosimeters used to measure dose distributions include ionization chamber, diode, film, and thermoluminescent dosimeter (TLD). They will be reviewed in this section. An overview of the various dosimetry techniques can also be found in the literature (Attix *et al.,* 1986, Johns and Cunningham, 1983).

### 1.2.1 Ionization Chamber

The ionization chamber is a highly precise dosimeter that is widely used in the field of radiotherapy. The chamber consists of a gas, usually air, and two electrodes which are responsible for collecting the ions created in the gas. The traditional ionization chamber is the thimble chamber, which has a central electrode surrounded by wall material. The molecules of the gas are ionized by an incoming radiation beam. Ion pairs arise from this ionization, the positive ions being collected on the negative electrode and the negative ions being collected on the positive electrode. The amount of charge collected is proportional to the amount of radiation that is imparted. A voltage is the order of a few hundred unit must be applied across the electrodes in order for the ion pairs to be collected, due to the tendency of the ion pairs to recombine when there is little or no voltage.

The efficiency of the dosimeter increases as the amount of recombination decreases. The amount of charge produced by the chamber is proportional to the energy absorbed in the chamber. Over a wide range of photo/electron energies, the ratio of energy per unit charge, known as (W/e), is found experimentally to be 33.97 J $C^{-1}$ in air. This allows for accurate measurement of dose. An added advantage of this dosimeter is that air cavity is nearly tissue equivalent. This does not suggest that corrections for air cavities such as those found in the human body should be ignored because the size of the ionization chamber air cavity is small. 0.1 - 0.3 $cm^3$, and therefore is said not to disrupt the photon fluency in the medium.

For use of these chambers at high energies, a build-up cap is placed over the chamber. Made out of material that is similar to tissue, this build-up cap aid in the establishment of electronic equilibrium, the thickness of the build-up cap depends on the energy of the incident beam. Ionization chambers are used as the "standard" against which most other dosimetry techniques are calibrated.

### 1.2.2 Thermoluminescent Dosimeters

Thermoluminescent dosimeters, TLDs, are mainly composed of lithium fluoride in two major forms: powder and shaped solids. At the atomic level, the lithium fluoride atoms form a crystalline pattern which is called a crystal lattice. The electrons are shared in this lattice pattern, and when exposed to irradiation the electrons move from their atomic location to locations called traps, where they remain trapped until the dosimeter is heated. When the electrons are released through the heating process, they travel to the conduction band and then fall to their lattice ground states, emitting light.

This light is measured by a photomultiplier tube in units of electric charge and is proportional to the amount of radiation that was absorbed, expressed in cGy. TLDs may be reused but at the cost of losing the information; consequently, they can only be read out once. Benefits of TLDs are that they are nearly independent of dose-rate and have a wide dynamic range. Also Lif TLDs nearly tissue equivalent. For patient monitoring in Radiotherapy, the typical size of a TLD shaped into a chip is 3 mm x 3 mm x 1/2 mm.

### 1.2.3 Film

Film, also known as photographic emulsions, consists of microscopic grains of silver bromide dispersed in a gelatin layer on either or both sides of a supporting film. The reaction that takes place when a beam is incident on film is that $Ag^+$ ions are converted to Ag atoms. A latent image is produced and now the film is ready to be developed. During the developing process all remaining ions are reduced to silver atoms and the bromine is removed. The grains that have the latent image will have the ions reduced more rapidly. What is left is opaque silver that can be measured optically. Optical density (OD) is the parameter obtained from the transmission of light through the film and which is related to dose. Some advantages of film are that it has good spatial resolution, is dose-rate independent, and is easily obtained commercially.

Some major disadvantages of film are that it has a strong dependence on the incident energy due the high Z of the material, the film batch and the processor. The high Z of film increases the probability of photoelectric absorption occurring at low energies. Furthermore, air gaps can arise when placing film in a phantom and cause inaccuracies in measuring dose.

### 1.2.4 Diodes

Diodes, also known as semiconductor dosimeters, are solid state devices that measure dose and dose rate. The most common diodes used are silicon diodes with *p-i-n* junctions. The p region is where holes are located, the *i* region is called the intrinsic region, and the n region is where excess electrons are located.

The diode is used either in a reversed-bias or an unbiased state. The incident radiation creates electron-hole pairs. The electrons are then elevated to the conduction band while the holes are left in the valence band. The resulting current which is related to the dose rate is measured by an electrometer. The signal that is produced when the radiation is applied is approximately 10 this greater than that produced in an ion chamber. This is due to the small amount of energy required to produce an ion pair (W/e), the high density of the material and high atomic number (Z).

Unfortunately, like film, diodes have energy dependence and therefore must be calibrated against an ion chamber. The advantages of diodes are that they have good spatial resolution and like TLDs can be placed on the skin of patients to measure localized surface doses. But unlike TLDs, diodes are able to read and display the dose in real time. These detectors can be used for both photons and electrons, but there is a different design for the two types of radiation fields. For electrons, the p-type diode, where the holes are the majority carrier and dominate the electrical conductivity, is used in dosimetry (Attix, 1986).

## 1.3 Gel Dosimetry

Modern radiotherapy techniques such as conformal radiotherapy (stereotactic radiosurgery, stereotactic radiotherapy and intensity modulated radiotherapy (IMRT)) are designed to deliver highly conformal radiation doses to tumours whilst sparing nearby sensitive tissues from overly large doses. These procedure require complicated dose calculation based on imaging data and the treatment planing computer alogrithms. To verify the accuracy of these techniques the three dimensional (3D) radiation dose distribution must be measured before treatment. Dosimeters such as ionization chambers and thermoluminescent devices have limitations in that they only measure the dose at a point, and radiographic films could only measure a 2 dimensional (2D) dose distribution.

Recently the polymer gel dosimetry has been shown to have potential in giving three dimensioned dose information with sub-mm spatial resolution. Gel dosimeters consist of a gel infused with radiation sensitive materials. After irradiation a measurable change is induced in the active materials which are held in position by the gel matrix, thus preserving a spatial record of the irradiation.

The gel usually consists of water mixed with a gelling agent such as gelatin, agarose or polyvinyl alcohol (PVA). Not only are they a 3D dosimeter, but the dosimeter itself is shown to be tissue equivalent phantom and hence does not perturb the dose distribution resulting in more accurate radiation dose distribution measurement. Because gels are manufactured as a liquid they could be poured into containers of varying shape for dosimetry purposes.

The biggest challenge in gel dosimetry at present is to extract dose information from the irradiated gel dosimeter. Various methods have been proposed to extract the dose distribution from irradiated polymer gel including megnatic resonance imaging (MRI) (Maryanski *et al.*, 1994a), optical computed tomography (OCT) (Gore *et al.*, 1996, Maryanski *et al.*, 1996), Raman spectroscopy (Baldock *et al.*, 1998a), X-ray computed tomography (CT) (Hilts *et al.*, 2000) and ultrasound (US) (Mather *et al.*, 2002b).

### 1.3.1 Historical Overview of gel dosimeter

Since 1984 there has been a proliferation of research into gel dosimetry from groups throughout the world. In 1999 the First International Workshop on Radiation Therapy Gel Dosimetry (DOSGEL'99) took place in Lexington, USA and in 2001 the 2$^{nd}$ International Conference on Radiation Gel Dosimetry took place in Brisbane, Australia. A third conference has been in 2004 at the International Atomic Energy Agency in Vienna, Austria. The 4$^{th}$ International conference on radiotherapy Gel dosimeter has been in 2006 at Ghent University in Ghent, Belgium.

Radiation-sensitive gels were first developed in the 1950s when Day and Stein investigated a color change upon irradiation of a gel containing Folin's phenol (Day *et al.*, 1950). It was later observed that irradiation induces polymerization in crystalline acrylamide (Mesrobian *et al.*, 1954). In 1957, Andrews et al. made measurements of photon and electron depth doses using Fricke and agarose gel (Andrews *et al.*, 1957). Later studies were done which utilized Fricke solutions and gels, and in 1958, Hoecker and Watkins studied an alternative method. This method was based on radiation-induced polymerization in monomer and gel solution (McJury *et al.*, 2000).

### 1.3.1.1 Frick gel

The proposed method uses the Fricke ferrous sulphate chemical dosimeter solution (Fricke *et al.,* 1927). The conversion of ferrous ($Fe^{2+}$) to ferric ions by ionizing radiation alters the magnetic moment of the metal ion. As a result, the spin relaxation times (T1 and T2) of the hydrogen nuclei in the aqueous gel are reduced. To obtain a gel, gelatin, agarose and sephadex G-200 were used as gelling substances (Gore *et al.*, 1984; Hiraoka *et al.,* 1986).

Several basic experimental studies were performed on Fricke gels investigating the effect of the gelling substances and the relation between dose and sensitivity of ferrous sulphate concentration (Hazle *et al.,* 1991; Olsson *et al.,* 1992a) and the relaxation mechanism at different field strengths (Rousseau *el at.,* 1994; Duzenli *et al.,* 1994). It was shown that adding a metal ion indicator such as xylenol orange induces color changes in the gel upon irradiation enabling the gel to be scanned optically (Appleby *et al.,* 1991). From theoretical considerations, it is shown that the Fricke gels (agarose, gelatin and xylenol doped gels) are water equivalent in the therapy range of electron and photon energies (Kron *et al.,* 1994; Chan *et al.,* 1995).

A limitation in Fricke gel dosimeters is that the ferric ions diffuse throughout the gel leading to degradation in spatial dose information within hours of irradiation (Olsson *et al.,* 1992b). In 1993 and 1994 Maryanski *et al.* published two papers reporting investigation of a gel infused with radiation sensitive polymers which give rise to an MRI signal after irradiation, and which does not suffer the diffusion problems of Fricke gel dosimeters (Maryanski *el al.,* 1993, 1994b).

### 1.3.1.2 Polymer Gel Dosimeters

Polymer gel dosimeters consist of monomers mixed into a gel solution. The most widely used monomer to date has been Acrylamide (AA) mixed with the cross linker N,N'-methylene-bis-acrylamide (BIS) (Maryanski *et al.,* 1993) although other chemicals have been used such as 1-vinyl-2-pyrrolidinone (Pappas *et al.*,1999) and 2-Hydroxyethylacrylate (HEA) (Lepage *et al.*,2001a).

Upon irradiation free radicals released during the radiolysis of the water within the gel initiate polymerization and cross-linking of the monomers. The amount of free radicals released is proportional to the dose received by the gel dosimeter and the resultant amount of polymer formed is therefore also proportional to dose until an upper limit is reached. After the upper dose limit is reached consumption of monomers results in a saturation effect (Baldock *et al.,* 1998a).

Oxygen is an efficient scavenger of free radicals and must be removed from polymer gel dosimeters prior to irradiation or the polymerization process will be inhibited (De Deene *et al.,* 2001; Salomons *et al.,* 2002).This results in the requirement for specialized equipment, manufacturing procedures and post-manufacture handling and has been a disadvantage of using polymer gel dosimeters.

Production of polymer gel dosimeters is achieved either by sealing the chemicals in mixing flasks and flushing the gel and flask with nitrogen followed by pumping the gel from the preparation flask into the phantom (Maryanski *et al.*, 1994a; Baldock *et al.*, 1998b), or by enclosing the chemicals and phantom in a glovebox flushed with nitrogen or argon and completely preparing the polymer gel dosimeter within.

Mixing procedures for gelatin gels normally involve soaking the gelatin in water and heating to approximately 50°C under continual stirring followed by adding the monomers and stirring until they are dissolved (Baldock *et al.*, 1998b). For agarose gels the same procedures are followed however the water and agarose mixture is heated to above 90°C to allow the agarose to mix with the water and the solution is then cooled to 50°C before adding the monomers. After the gel dosimeter is mixed it is poured into a phantom before gelation occurs.

After a polymer gel dosimeter is manufactured it must remain oxygen free until it is irradiated and polymerization has occurred. Phantom wall materials must therefore have a low permeability to oxygen. Plastic and Perspex phantoms show signs that oxygen can penetrate into the gel and degrade the dose information (Maryanski *et al.*, 1994a) whereas glass and Barex (BP Chemicals) have shown to have low oxygen permeability for the purposes of polymer gel dosimetry (Bonnett *et al.*, 1999; Baldock *et al.*, 1996).

Although these polymer gel dosimeters above have been validated in some clinical applications, their use in the clinic has been limited. One of the reasons is the laborious manufacturing process especially due to the procedure of avoiding oxygen to infiltrate the gel. Attempts have been made to decrease the sensitivity to oxygen by binding the oxygen in metallo-organic complexes. Although some oxygen effects may still be encountered, these new normoxic gels are very promising as gel dosimeters, the first normoxic gel, known by the name MAGIC gel (Fong *et al.*, 2001).

Based on the recommendation from previous works (De Deen *et al.*, 2002a; Venning *et al.*, 2005) the characteristics of good polymer gel as dosimetry are:

1. It must be tissue or water equivalent, as the dosimeter itself must not perturb the dose distribution.

2. It must have a linear dose response over a clinically useful range.

3. The dosimeter must be stable for a sufficiently long period to enable irradiation and dose analysis.

4. The dosimeter must remain stable during shipment, unaffected by a variety of environmental conditions throughout the analysis period.

6. It must be no toxicity in polymer gel.

### 1.3.1.3 MAGIC polymer gel

In 2001 Fong *et al.* investigated and reported a new polymer gel formulation which contains oxygen scavengers and can be manufactured in normal atmospheric conditions, thus greatly simplifying the production to the point that polymer gel dosimeters can now be made on the bench top without the requirement to purchase specialized equipment This formulation consists of methacrylic acid, copper sulphate, ascorbic acid, hydroquinone, gelatin and water and is given the acronym MAGIC (Fong *et al.,* 2001).It is expected that this development is a major step towards the widespread clinical use of gel dosimeters.

### 1.3.1.3(a) MAGIC gel chemical reactions

The result of present study showed that the MAGIC gel is an aqueous solution of gelatin mixed with methacrylic acid (MAA), copper sulphate and ascorbic acid (AA). The principles of the polymerization are expected to be similar kind to the dosimeter gel, though there is gelatin present. A kinetic study of the polymerization of methyl acrylate in aqueous medium containing oxygen, ascorbic acid and copper (II) has been reported (Gangi *et al.,* 1982).

### 1.3.1.3(b) Reaction mechanisms

It is believed that the complex of Cu (II), ascorbic acid and oxygen with radiolysis of water serves as a free radical source for the initiation of the polymerisation of methacrylic acid (De Deen *et al.,* 2002a).

$O_2 + AA + Cu^{2+} <=> (complex)$, irradiation => R

These free radicals (R) can react with monomers (M) and form monomer radicals ($M^*$), (initiation), it is also likely that formation of gelatin radicals take place. This step is followed by propagation or termination, where the propagation involves creation of polymer radicals, and the termination occur when two polymer radicals neutralize each other or a polymer radical reacts with Cu (II) and the chain propagation stops (Gangi *et al.,* 1982).

Initiation: $R + M \Rightarrow M_1^*$

Propagation: $M_{(n-1)} + M \Rightarrow M_n^*$

Termination: $M_n^* + M_n^* \Rightarrow$ polymer

$M_n^* + Cu\ (II) \Rightarrow$ polymer + Cu (I)

It is also believed that molecules of the gelatin can terminate polymerization.

## 1.4 Imaging of the polymer gel dosimeter

One of the factors impeding the routine use of polymer gel dosimeters clinically has been the difficulty involved in extracting accurate dose information through medical imaging techniques. There are a number of methods used to extract dose information from gel dosimeters.

### 1.4.1 MR relaxation time imaging

The main imaging modality of choice to date has been magnetic resonance imaging (MRI) (Fong *et al.*, 2001; De Deene *et al.*, 2002a; De Deene *et al.*, 2002b; Gustavsson *et al.*, 2003; Scheib *et al.*,2004; Amin *et al.*, 2004; Gear *et al.*,2006).

MRI allows the measurement of the longitudinal and transverse relaxation rates (R1 and R2) of the dosimeter gels, from which dose maps can be calculated. Conventionally, the corresponding relaxation times (T1 and T2) are measured, from which the rates can be computed. Relaxation times are measured by applying radiofrequency (RF) pulses to excite the magnetization of the spin system, and then sampling during the return to equilibrium.

The transverse relaxation time T2 (=1/R2) is measured by fitting data collected from at least two points on the transverse relaxation curve following excitation. Two main approaches to data collection are used (a) Single echo or Hahn spin echo sequence method. (b) Multiple spin echo method (Baustert *et al.*, 2000). MRI was the method used by Maryanski *et al.* (1994b) and has resulted in the most research activity to date. The amount of polymerization is related to the absorbed dose (Maryanski *et al.*, 1996).

The transverse relaxation time, *T2* is temperature sensitive, which means that polymer gel dosimeters evaluated by this method must be brought to a stable temperature prior to imaging (Maryanski *et al.,* 1997). Temperature drift in the polymer gel dosimeter during imaging can cause a change in *T2* (De Deene and De Wagter, 1999). Also the image plane inhomogeneities and lengthy imaging times are included in the current limitations of MRI (Oldham *et al.,* 2001).

### 1.4.2 Optical CT imaging (OCT)

Much research effort is being conducted into developing alternative methods to image the dose distribution recorded in gel dosimeters. Techniques are being investigated to find imaging techniques with less inherent noise than MRI and to eliminate reliance on MR technology with its associated issues of limited access and high scanning cost (Oldham *et al.,* 2001).

Polymer gels can be easily visualized upon irradiation due to their opalescent appearance as the radiation dose increases (Oldham *et al.,* 2001, 2003). Qualitative testing can thus be done by visual inspection or through the use of an optical densitometer (Maryanski *et al.,* 1996; Rae *et al.*, 1996). McJury *et al.* (2000) performed an investigation that utilized optical scanning as an imaging technique. Due to the increase in opacity of the gel upon irradiation, they determined that it is possible to use the optical scanning technique to generate a two-dimensional dose distribution. Light attenuation was found to be related to polymer density and thus absorbed dose, with the understanding that light within a BANG-1 gel is scattered rather than absorbed by the polymer particles.

Oldham *et al.* (2001) performed a study on the effectiveness of gel dosimetry and optical-CT (computerized tomography) scanning as a verification method for complex radiosurgery deliveries and by extension IMRT deliveries. As the laser was stepped in increments of 1 mm across the flask, horizontal line scans were taken. A total of 100 projections were acquired which corresponded to 180 degrees of projection data. The paper demonstrated that the optical-CT scanning method for BANG-3 gels yielded 2D dose distribution with good resolution.

The major applications of dosimetry using OCT have been for brachytherapy. External beam treatments on large samples represent a challenge for the OCT method because of the large pathlengths through the sample. This results in considerable signal attenuation, requiring a high sensitivity and dynamic range in the detector (Doran *et al.*, 2001).

### 1.4.3 Ultrasound

Mather *et al.* (2001, 2002a) showed that ultrasound could be used to investigate changes in irradiated PAG polymer gels. In these studies, acoustic speed of propagation, attenuation and transmitted signal intensity showed a strong variation with absorbed dose indicating the potential of this technique.

Comparative studies of PAG and MAGIC polymer gels indicated that differences in acoustic properties with absorbed dose were due to differences in the elastic modulus of the materials (Mather *et al.*, 2002b). Further acoustic studies showed that the overall acoustic attenuation, dose sensitivity and dynamic range were dependant on dosimeter formulation (Mather *et al.*, 2003a).